

# Performance Analysis of Four Plant Fiber/Polyvinyl Chloride Composites under Two Degradation Conditions with Water or Seawater with Xenon Lamp

Xinyu Zhong,<sup>a,b</sup> Yaowen Zhu,<sup>a,b</sup> Shuaijun Liu,<sup>a,b</sup> Jingjing Fu,<sup>c</sup> Hong Lin,<sup>a</sup> and Chunxia He<sup>a,b</sup>\*

To explore the properties of wood-plastic composites (WPCs) used in maritime climates, four different plant fibers (bamboo, rice straw, wheat straw, reed straw), and polyvinyl chloride (PVC) were used to prepare WPCs through extrusion. The composites were subjected to either seawater immersion + xenon lamp aging or deionized water spray + xenon lamp aging. The mechanical properties (tensile strength, flexural strength, impact strength), color change, and water absorption performance were analyzed. The plant fibers were analyzed by X-ray diffraction and Fourier transform infrared spectroscopy (FTIR), and the microstructures of the surfaces were observed by scanning electron microscopy (SEM). The reed fiber had the highest crystallinity; reed/PVC composites had good interface with the plastic matrix, less internal defects, and the best comprehensive performance, with a tensile strength, bending strength, and impact strength of 25.4 MPa, 34.4 MPa, and 4.30 KJ·m<sup>-2</sup>, respectively. The simulated seawater immersion + xenon lamp aging reduced the performance of wood-plastic composites, destroyed the quality of the combination of plant fibers and plastic matrix, and created internal defects. The comprehensive mechanical properties of reed/PVC composites were the best. The properties of bamboo/PVC composites decreased the least, with a decrease of less than 41.2%.

*Keywords:* Plant fibers; Polyvinyl chloride; Wood-plastic composites; Simulated seawater degradation; Xenon lamp aging

*Contact information:* a: College of Engineering, Nanjing Agricultural University, Nanjing 210031, China; b: Key Laboratory of Intelligence Agricultural Equipment of Jiangsu Province, Nanjing 210031, China; c: Nanjing Research Institute for Agricultural Mechanization, Ministry of Agriculture and Rural Affairs; \* Corresponding author: chunxiahe@tom.com

## INTRODUCTION

Wood-plastic composites (WPCs) are not only eco-friendly but also have good mechanical properties and good processing performance. They have been widely used in outdoor walkway boards, garden construction, logistics packaging, *etc.* (Hao and Wang 2016; You 2016; Ye 2018). However, they also reveal some disadvantages of plastics and plant fibers. Plastics exposed to sunlight are prone to aging; plant fibers are susceptible to degradation when exposed to water or a humid environment. Both of these phenomena reduce the performance of the composites (Pan *et al.* 2013). Currently, WPCs are increasingly used in marine industry and commercial applications. When exposed to the outdoor and degradative medium, WPCs experience performance degradation and internal structural damage, such as matrix plasticization and surface blistering (Segovia *et al.* 2007). Therefore, it is of great significance to study the solar aging resistance and resistance of

degradative water conditions of the WPCs.

Scholars within China and abroad have carried out some studies on the performance of WPCs when used outdoors. Due to photooxidation and photodegradation, the mechanical properties of WPCs are degraded, and the appearance becomes faded when exposed for a long time to sunlight. Solar radiation is a significant factor that affects the service life of WPCs in outdoor applications. Humidity or aqueous environments such as rivers or oceans also influence the performance of WPCs. The existing literature has only focused on the performance of WPCs under single conditions. For solar radiation, Xiao and Li (2010) found that the flexural strength and elastic modulus of wood flour/high-density polyvinyl chloride (HDPE) and rice hull/high-density PVC composites decrease with prolonged aging time in the accelerated aging test of xenon lamps. Deka *et al.* (2012) researched the wood polymer nanocomposite (WPNC), which was developed by using high-density polyethylene (HDPE), low-density polyethylene (LDPE), polypropylene (PP), polyvinyl chloride (PVC), wood flour (WF), polyethylene-co-glycidyl methacrylate PE-co-GMA), and different nanoparticles, *viz.* nanoclay, SiO<sub>2</sub>, and ZnO. The results of the study with X-ray diffraction (XRD) showed that WPC loaded with nanoclay, SiO<sub>2</sub>, and ZnO had improved flammability, chemical resistance, and UV resistance. Hou *et al.* (2013) conducted natural aging experiments on wheat straw/polypropylene (PP) composites, finding that the tensile, flexural, and impact strength of wheat straw/PP composites decreased first and then became stabilized with increasing aging time. Qi *et al.* (2019) studied the influences of the acrylate-styrene-acrylonitrile (ASA) modification on the aging behavior of eucalyptus/polyvinyl chloride (PVC) composites with xenon lamp aging conditions, and the FTIR results manifested the physical and mechanical properties of the composites deteriorated. Zor *et al.* (2019) investigated the effect of heat-treated lignocellulosic filler on the surface characteristics and decay resistance of the wood flour/styrene maleic anhydride (SMA) composites. Weathering tests were carried out by UV-light irradiation. The results of FTIR indicated that the increase in wood filler reduced the resistance to the weathering. The ultraviolet in natural light excites the C-H bond, which reacts with oxygen to generate peroxide and cracks the surfaces of WPCs. There have been fewer studies on the performance of WPCs in seawater. Najafi and Kordkheili (2011) researched the influences of the seawater in the Caspian Sea and Persian Gulf on the physical and mechanical properties of wood powder/polypropylene (PP) composites. Seawater with higher salinity causes greater degradation of the physical and mechanical properties of the composites. Jiang *et al.* (2019) tested the properties of four different plant fibers (eucalyptus, poplar, bamboo, and rice husk) reinforced high-density polyethylene (HDPE) composites under the simulated seawater with accelerated degradation. The deterioration of the interface of two-phase, mechanical properties, and color change of the four types of WPCs were attributed to the degradation of simulated seawater. Fu *et al.* (2019) has investigated the resistance of eucalyptus (EU) reinforced high polyethylene (HDPE) composites when exposed in simulated seawater. The EU fibers were modified by alkali treatment with NaOH. According to the FTIR analysis, the alkali treatment could strengthen the interface bounding force between the EU fiber and HDPE in terms of chemical structure level. Jiang *et al.* (2019) developed a new degradation and wear-resistant material by using polyvinyl chloride (PVC)/sorghum straw (SS) composites reinforced with micro-silica (MS) and poly(acrylonitrile-styrene-acrylate) (ASA). The simulated extreme cyclic degradation conditions were simulated by simulated seawater and acid rain. And the FTIR results indicated the ASA/MS (especially ASA) modification was contributed for higher water and moisture resistance. In the actual situation, WPCs are

affected by the solar radiation and water simultaneous when utilized outdoors, but there has been a lack of research related to that situation.

The objective of this study was to explore the performance of four kinds of plant fibers (bamboo powder, rice straw, wheat straw, and reed straw) reinforced polyvinyl chloride (PVC) composites under two types of degradation environments: 1.) immersion in the simulated seawater plus xenon lamp aging; 2.) deionized water spraying plus xenon aging. The effect of the fiber type on the X-ray diffraction (XRD), mechanical properties, water absorption, Fourier transform infrared spectroscopy (FTIR), and morphology of the composites under two different degradation conditions were investigated. The analysis of the degradation and aging mechanisms of four kinds of WPCs will promote their application in the marine industry and commercial fields.

## EXPERIMENTAL

### Materials

At present, the most easily available plant fibers are straw and bamboo plant fibers. In this paper, the four most common plant fibers were selected for research. Rice straw powder, wheat straw powder, and reed straw powder were purchased from Lianyungang, China. Bamboo powder was purchased from Lishui, China. The PVC and the Ca/Zn stabilizer were purchased from Shaoyang Paradise Auxiliary Co., Ltd. (Dongguan, China). The PE wax SQI-H108 was purchased from SQI, Nontaburi, Thailand. The Malay grafted PVC (Grade A, 150,000 molecular weight) was purchased from LG Korea, Busan, Korea.

### Wood Plastic Composite Preparation

The air-dried plant fibers were completely crushed and ground so that they could be divided with a 100-mesh screen to get 100-mesh fiber powder. Screened plant fibers were dried at 90 °C for 12 h in a DHG-9140A electro-thermostatic drum-wind drying oven (Nanjing Dongmai Scientific Instrument CO., Ltd., Nanjing, China) to eliminate moisture.

The dried plant fibers, PVC, Ca/Zn stabilizer, PE wax, and Malay grafted PVC (43 wt%, 43 wt%, 7 wt%, 4 wt%, and 3 wt%, respectively) were mixed in the SBH-5L 3D linkage mixer (Nanjing Xinbao Mechanical and Electrical Industry Co., Ltd., Nanjing, China). The speed of the mixer was set to 30r/min.

Extrusion of four composite materials was carried out using an RM200C conical twin-screw base platform (Harbin Harper Electric Co., Ltd., Harbin, China). During the extrusion, the temperature of the four processing zones were 150, 155, 160, and 165 °C, respectively. The head pressure was set 0.5 MPa, and the rotational speed of the screw was 20 rpm. The material was demolded into strips according to the test standard, with a width of about 10 mm, a thickness of 7 mm, and a length of 10 cm.

### Wood Plastic Composite Degradation Aging Experiment

To simulate the degradation aging of wood-plastic composites under actual conditions, including the degradation aging of composite materials in sunlight and sea water and the alternating action of sunlight and rain, two methods were adopted.

In the simulated seawater immersion + xenon lamp degradation aging experiment, the four types of plant fiber/PVC composite materials were treated with different aging methods and aging times. As shown in Table 1, the four types of plant fiber/PVC composite materials were immersed in simulated seawater and placed in an ASTM-type xenon lamp

aging test box (Kewen Environmental Testing Equipment Co, Ltd., Dongguan, China). In order to accelerate the aging of wood-plastic composite materials and shorten the experimental period, the temperature was maintained at  $60 \pm 1$  °C. The illumination time was set to 1 hour and 40 min. The dark time was 20 min and loop in this way. The treatment time was 3 days (first cycle), 6 days (two cycles), and 9 days (third cycle) to simulate the degradation aging of wood-plastic composites under the combined action of seawater and light when applied to the seaside plank road. There were 80 samples for experiment in each processing cycle for subsequent testing.

**Table 1.** Experimental Setup

Experiment	Simulated Seawater Immersion + Xenon Lamp Degradation Aging Experiment	Deionized Water Spray + Xenon Lamp Degradation Aging Experiment
Temperature setting	$60 \pm 1$ °C	$60 \pm 1$ °C
Number of samples	10 for each material	10 for each material
Fast aging cycle	120 min	120 min
Illumination time	100 min	100 min
Dark time	20 min	20 min
Processing method	Simulated seawater immersion	Deionized water spray in dark time
Processing time	3 days, 6days and 9days	3 days, 6days and 9days

The composition of simulated seawater is shown in Table 2 (Yu *et al.* 2011), where deionized water was used as the solvent. After preparation, an appropriate amount of NaOH was added to adjust the pH value of the simulated seawater to the weakly alkaline range to simulate the degradation aging under the interaction of light and rain during use.

**Table 2.** Chemical Components of Simulated Seawater

Component	NaCl	MgCl <sub>2</sub>	KCl	MgSO <sub>4</sub>	NaHCO <sub>3</sub>	CaCl <sub>2</sub>	NaBr
Concentration (g·L <sup>-2</sup> )	26.5	24	0.73	3.3	0.2	1.1	0.28

In the deionized water spray + xenon lamp degradation aging experiment, the four kinds of plant fiber/PVC composite materials were placed in the xenon lamp aging experiment box and kept at  $60 \pm 1$  °C. The illumination time was set to 1 hour and 40 min, and the dark time was 20 min while deionized water was sprayed. The treatment time was the same as the first experimental method.

### Performance Test

The tensile strength and flexural strength used a CMT6104 electronic universal testing machine (Meters Industrial Systems Co., Ltd., Shenzhen, China) at a loading speed of 2 mm/min according to standards GB/T 1040.1 (2006) and GB/T 9341 (2008). The impact strength test of the composites was tested by impact pendulum (Anhui Huabiao Testing Instrument Co., Ltd., Hefei, China) according to standard GB/T 1451 (2005). Before the start of the experiment, the samples were marked 2 cm from both ends, and the equipment applied force on the sample center. There were 10 samples of each material for each processing cycle, which were used to each performance test.

The water absorption test was performed using an HH-600 digital display constant temperature water tank (Shanghai Baidian Instrument Equipment Co., Ltd., Shanghai,

China). Referring to standard GB/T 17657 (2013), 10 samples of each composite material in each treatment cycle and the same sample that had not been aged but soaked for the same time were placed in a drying oven for 24 h for comparison, and they were put into the HH-600 digital display constant temperature water tank for 24 h. The temperature was maintained at  $35 \pm 1$  °C, and the average values were taken.

The color difference test, according to the CIE 1976  $L^*a^*b^*$  color system, was performed using an HP-200 precision color difference meter (Shanghai Hanpu Optoelectronics Technology Co., Ltd., Shanghai, China), which was used to test the color change of the surface of the material before and after the experiment. Lightness ( $L^*$ ) and chromaticity coordinates ( $a^*$  and  $b^*$ ) were measured for samples.  $L^*$  represents the lightness coordinate and varies from 100 (white) to 0 (dark);  $a^*$  represents the red ( $+\Delta a^*$ ) to green ( $-\Delta a^*$ ) coordinate;  $b^*$  represents the yellow ( $+\Delta b^*$ ) to blue ( $-\Delta b^*$ ) coordinate. There were 10 samples of each material for each processing cycle, and each sample was tested 6 times at different positions. The results were the average of the measurement results. The color difference was calculated by Eq. 1,

$$\Delta E = [(\Delta L^*)^2 + (\Delta a^*)^2 + (\Delta b^*)^2]^{1/2} \quad (1)$$

where  $\Delta E$  is the color difference;  $+\Delta L^*$  and  $-\Delta L^*$  represent whitening and darkening, respectively;  $+\Delta a^*$  and  $-\Delta a^*$  represent the color shift toward red and green, respectively;  $+\Delta b^*$  and  $-\Delta b^*$  represent the color shift toward yellow and blue, respectively.

The chemical structures of the four types WPCs were characterized using a Nicoletis-10 FTIR spectrometer (Thermo Fisher Scientific, Shanghai, China). The samples after aging were ground into a powder and mixed with KBr for tableting. During the measurement, the tablet was loaded into the tablet clamp, and the KBr blank tablet was used as a reference to scan the infrared spectrum. There were 10 samples of each material for each processing cycle, and each result was the average of them. The measurements were performed from 400 to 4000  $\text{cm}^{-1}$ , with a resolution of 4  $\text{cm}^{-1}$ , and each spectrum was collected from 16 scans in the absorbance mode.

The crystal structures of the straw fibers were characterized using an X'Pert PRO X-ray diffractometer (XRD, Analytical B.V., Almelo, Netherlands) with a Cu K  $\alpha$  radiation source ( $\lambda = 1.54056$ ), at an accelerating voltage of 40 KV and applied current of 40 mA. The plant fiber powder was placed in a container and flattened, then tested with a diffractometer. The performance test is tested 3 times and averaged. The specimens were scanned at a speed of 0.33°/min, with  $2\theta$  ranging from 10 to 90°. The crystallinity index (CrI) was calculated using the following formula,

$$CrI = (1 - I_{am}/I_{002}) \times 100\% \quad (2)$$

where  $I_{002}$  is the intensity of the crystalline phase ( $2\theta = 22.5^\circ$ ), which essentially consists of cellulose substances, and  $I_{am}$  is the intensity of the amorphous phase ( $2\theta = 18^\circ$ ), which represents the hemicellulose and lignin substances.

Morphological analyses of the stretch sections before and after experiments were performed using an S-4800 scanning electron microscope (SEM, Hitachi, Tokyo, Japan). Ten samples of each tensile fracture were tested.

## RESULTS AND DISCUSSION

### Crystallinity Analysis of Wood Fiber Composite Plant Fiber

Figure 1 shows the XRD patterns of four wood-plastic composites. The X-ray diffraction patterns of the four plant fibers all have peaks around  $2\theta = 16^\circ$  and  $22^\circ$ , and the difference is in the peak value,  $2\theta = 16^\circ$ . The peak value is related to the presence of lignin and hemicellulose. The peak at  $2\theta = 22^\circ$  is related to the presence of cellulose molecules (Rouhou *et al.* 2018). Cellulose is the crystalline phase in plant fibers, and the plant fiber specific gravity is higher the higher when the crystallinity of plant fibers is higher.

The crystallinity of the four plant fibers calculated according to Eq. 2 is shown in Table 3. The chemical composition of the four plant fibers is shown in Table 4, which is based on measurements by Van Soest washing fiber analysis. Among the four plant fibers, the reed fiber had the highest crystallinity (52.7%) and the rice straw fiber had the lowest crystallinity (41.7%). The difference in fiber crystallinity was due to the chemical composition and structure of different plant fibers.

According to the analysis, the cellulose was within crystalline phases, and its molecular arrangement was regular. The hydroxyl reactivity was lower than that of the non-crystalline phase. A higher crystallinity indicates a less reactive hydroxyl group, resulting in a lower surface polarity of the plant fiber. With a higher interfacial strength between the matrix and plant fiber of wood-plastic composites formed by plant fibers (Li 2013), there are less internal defects, which can provide a certain positive correlation with the mechanical properties, water absorption properties.

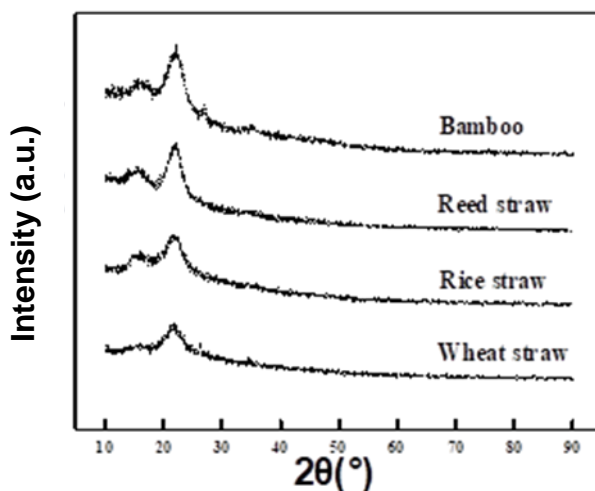


Fig. 1. XRD maps of four plant fibers

Table 3. Crystallinity of Four Wood-plastic Composites

Plant fiber type	Wheat straw	Rice straw	Reed	Bamboo
Crystallinity (%)	45.34	41.67	52.66	46.84

**Table 4.** Plant Fiber Chemical Composition

Fiber	Cellulose (%)	Hemicellulose (%)	Lignin (%)	Ash (%)
Wheat straw	44.64	20.15	17.04	4.42
Rice straw	42.73	22.09	13.54	3.11
Reed	46.57	21.23	19.21	1.21
bamboo	49.68	20.86	16.45	2.71

### Mechanical Properties of Wood-plastic Composites after Degradation Aging

Figure 2 shows the mechanical properties of four wood-plastic composites before and after degradation aging. The reed/PVC composites had the best mechanical properties before degradation aging, and their tensile strength, flexural strength, and impact strength were 25.4 MPa, 34.4 MPa, and 4.30 KJ·m<sup>-2</sup>, respectively. The mechanical properties of wheat straw/PVC composites and bamboo powder/PVC composites were similar to and slightly lower than that of reed/PVC composites. The mechanical properties of straw/PVC composites were the worst. After simulated seawater immersion + xenon lamp and deionized water spray + xenon lamp, the mechanical properties of the four wood-plastic composites decreased, and a longer degradation aging time resulted in decreased mechanical properties.

After two kinds of degradation aging, the mechanical properties of the reed straw composites were the best. The tensile strength, flexural strength, and impact strength decreased by 41.3%, 33.7%, and 45.3% and 24.1%, 25.3%, and 38.7%, respectively, after simulated seawater immersion + xenon lamp and deionized water spray + xenon lamp experiments. The mechanical properties of bamboo powder/PVC composites decreased the least, and the mechanical properties were second only to the reed/PVC composites. After simulating two kinds of degradation aging, the tensile strength, bending strength, and impact strength decreased by 36.0%, 40.6%, 43.8%, and 17.9%, 30.0%, and 34.0%, respectively. The mechanical properties of wheat straw/PVC composites and rice straw/PVC composites were poor. The mechanical properties of rice straw/PVC composites decreased the most. The tensile strength, flexural strength, and impact strength decreased by 55.3%, 45.6%, and 53.4% and 35.1%, 41.0%, and 36.4%, respectively, after the two kinds of degradation aging.

A comparison of the simulated seawater immersion + xenon lamp degradation aging with the deionized water spray + xenon lamp degradation aging revealed that the mechanical properties of wood-plastic composites were lower after simulated seawater immersion + xenon lamp degradation aging. Xenon lamp aging and seawater degradation influenced the wood-plastic composites. Therefore, the specific wavelength of ultraviolet light in the xenon lamp easily breaks down the chemical bond of the PVC molecular chain (Li *et al.* 2014). At the same time, it photochemically reacts with the plant fiber to degrade the hemicellulose and to attenuate the mechanical interlocking effect between fibers and PVC and the attraction of molecules between two phases, which intensifies the formation of cracks in wood-plastic composites.

The components such as NaCl, MgCl<sub>2</sub>, and KCl in the simulated seawater enter the wood-plastic composite with the aqueous solution. After drying, the salt is abundantly present at the junction of plant fiber and PVC, which increases the free volume of the material and makes the molecular chains move more freely (Sun *et al.* 2005). The contact frequency between simulated seawater and plant fibers increases. Under the action of simulated seawater, plant fibers are easily swelled. The swelling leads to cracking of the

PVC coating the plant fibers, which causes a large number of cracks generating on the joint surface of the plant fiber and PVC. The microscopic morphology reflects that parts of plant fibers are separated from the plastic matrix under the influence of simulated seawater solution, resulting in holes (Fig. 5).

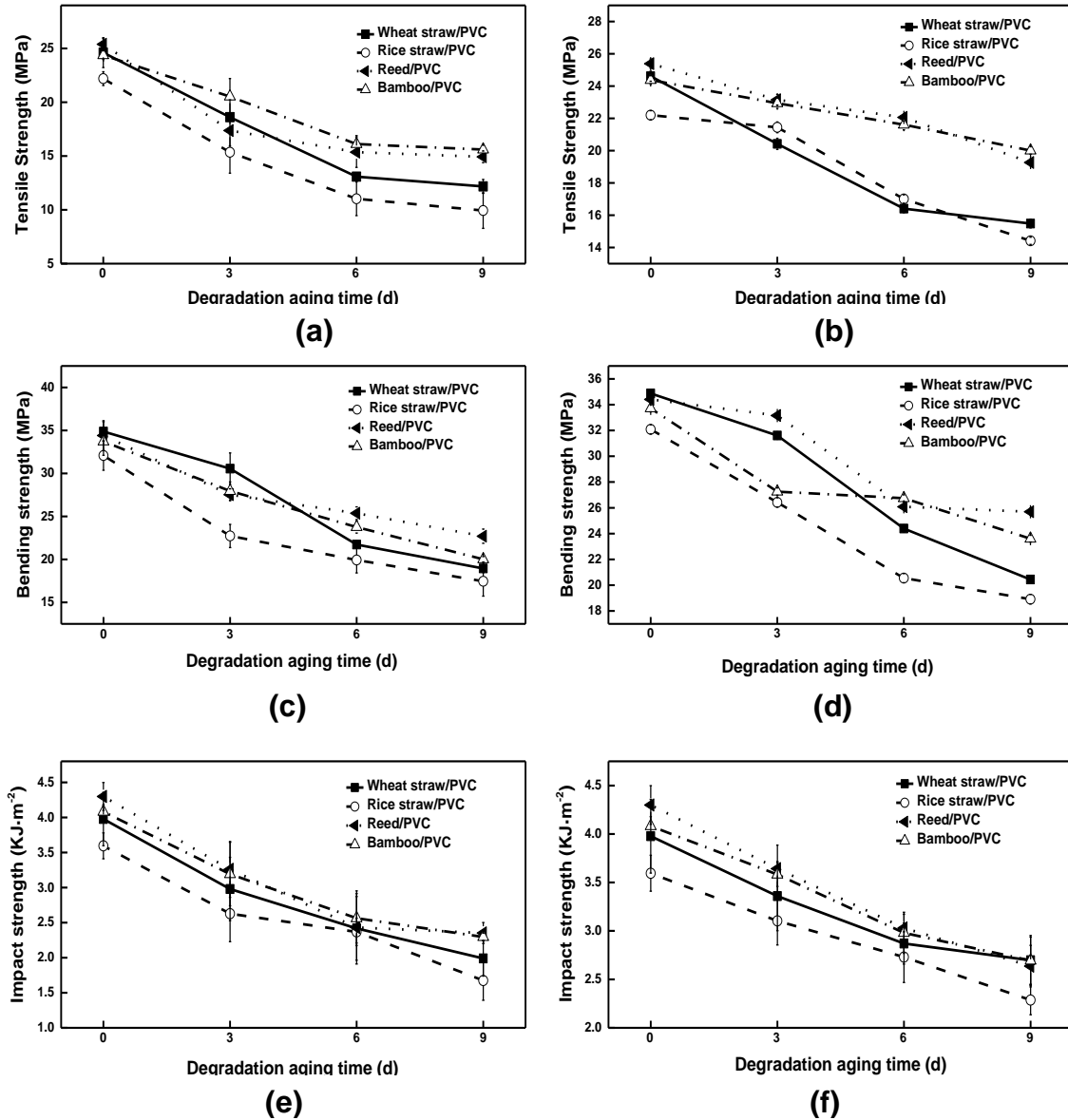


**Fig. 2.** Mechanical properties including tensile strength, bending strength and Impact strength after (a) (c) (e) simulated seawater immersion + xenon lamp degradation aging and (b) (d) (f) deionized water spray + xenon lamp degradation and aging.

The plant fiber content drops, which leads to stress concentration occurring at the defect when subjected to external force. Also, plant fibers become prone to fracture damage. In the deionized water spray + xenon lamp degradation aging experiment, the influence of wood-plastic composite materials is mainly caused by light aging. There is no simulated interaction between seawater degradation and aging of the xenon lamp. After the photochemical reaction, the plant fiber is not separated from the wood-plastic composite material, and the internal defects are mainly cracked on the joint surface of the plant fiber and PVC.

### Analysis of Color Difference after Degradation Aging of Wood-plastic Composites

Tables 5 and 6 show the change of color difference under two kinds of degradation conditions of four kinds of plant fiber/PVC composite materials. As the degradation aging time increased, the chromatic aberration of the wood-plastic composite increased, and the  $\Delta E$  value increased. As shown in Eq. 1, the factors affecting the change of  $\Delta E$  are  $\Delta L^*$ ,  $\Delta a^*$ , and  $\Delta b^*$ , wherein the main factor is  $\Delta L^*$ . That is, the color change was mainly the change of lightness, indicating that the four composite materials have obvious fading after degradation aging. The results are consistent with previous studies (Hou *et al.* 2014). After 9 days of degradation aging, the bamboo powder/PVC composite had the smallest color difference. The main reason is that the bamboo powder/PVC composite itself is light in color, therefore its color change was small after aging. The  $\Delta E$  values of the two different types of degradation aging after 9 days were 12.8 and 14.8, respectively. After deionized water spray + xenon lamp degradation aging, the color difference of reed/PVC, rice straw/PVC, and wheat straw/PVC composite was similar, and the  $\Delta E$  value was 35, among which the straw straw/PVC composite had the largest color difference in the simulated seawater. After simulated seawater immersion + xenon lamp degradation aging, the color difference of reed and rice straw/PVC composites was similar, and the  $\Delta E$  values were all around 38, while the wheat straw/PVC composites had the largest color difference. After 9 days of degradation aging, the  $\Delta E$  was 48.7.

A comparison of the deionized water spray + xenon lamp degradation aging and the simulated seawater immersion + xenon lamp degradation aging revealed that the color change of wood-plastic composite material was more obvious after simulated seawater immersion + xenon lamp degradation aging. Because PVC absorbs ultraviolet light and undergoes photooxidative decomposition, the chemical structures of polyenes and oxygen-containing groups are converted (Tang 1989), causing changes in strength and color. In addition, plant fibers absorb ultraviolet light to cause photochemical reactions, leading to the formation of aromatic and other free radicals, resulting in lignin degradation and photo-oxidation of cellulose and hemicellulose to produce chromatic aberration. Bamboo pink pigment content is low; the color change is relatively low. Simulated seawater immersion + xenon lamp degradation aging process caused many defects in the wood-plastic composite material. The simulated seawater contacted with the plant fiber without PVC coated to dissolve the fiber pigment in the seawater solution, causing serious color changes (Matuana *et al.* 2011). At the same time, the infrared spectra (Figs. 10 to 13) that in the 1500 to 1700  $\text{cm}^{-1}$  band and 1450 to 1600  $\text{cm}^{-1}$  band, the carbonyl and carbon-carbon bond of the benzene ring stretching vibration of the straw/PVC composite material and the reed/PVC composite material were strengthened. This result indicated that photochemical reactions occur under the aging effect of the xenon lamp to produce a chromophore group, which promotes color change.

**Table 5.** Variation of Color Difference of Four WPCs after Simulated Seawater Immersion + Xenon Lamp Degradation Aging

WPC Type	Processing Days (d)					
	3		6		9	
Wheat straw/PVC	$\Delta L^*$	14.25 ± 1.69	$\Delta L^*$	37.29 ± 2.32	$\Delta L^*$	48.13 ± 2.23
	$\Delta a^*$	7.25 ± 0.78	$\Delta a^*$	3.74 ± 0.27	$\Delta a^*$	3.39 ± 0.76
	$\Delta b^*$	7.11 ± 2.77	$\Delta b^*$	5.30 ± 0.38	$\Delta b^*$	6.09 ± 0.79
	$\Delta E$	17.79 ± 3.43	$\Delta E$	37.85 ± 2.24	$\Delta E$	48.65 ± 2.09
Rice straw/PVC	$\Delta L^*$	24.36 ± 2.67	$\Delta L^*$	24.86 ± 2.47	$\Delta L^*$	37.08 ± 1.97
	$\Delta a^*$	-3.46 ± 0.57	$\Delta a^*$	-4.11 ± 0.38	$\Delta a^*$	-5.06 ± 0.9
	$\Delta b^*$	-10.10 ± 0.91	$\Delta b^*$	-10.26 ± 0.53	$\Delta b^*$	-11.20 ± 1.30
	$\Delta E$	24.61 ± 2.80	$\Delta E$	27.25 ± 2.18	$\Delta E$	39.09 ± 1.97
Reed/PVC	$\Delta L^*$	21.82 ± 2.37	$\Delta L^*$	30.68 ± 0.7	$\Delta L^*$	36.82 ± 1.2
	$\Delta a^*$	3.85 ± 0.74	$\Delta a^*$	3.88 ± 0.1	$\Delta a^*$	2.80 ± 0.55
	$\Delta b^*$	-9.43 ± 0.82	$\Delta b^*$	-9.42 ± 0.51	$\Delta b^*$	-10.37 ± 0.95
	$\Delta E$	24.29 ± 2.07	$\Delta E$	32.33 ± 0.79	$\Delta E$	38.37 ± 1.34
Bamboo/PVC	$\Delta L^*$	6.53 ± 3.29	$\Delta L^*$	10.83 ± 1.46	$\Delta L^*$	13.81 ± 1.75
	$\Delta a^*$	-0.28 ± 0.19	$\Delta a^*$	-0.86 ± 0.44	$\Delta a^*$	-1.60 ± 1.73
	$\Delta b^*$	-5.79 ± 0.24	$\Delta b^*$	-4.11 ± 0.35	$\Delta b^*$	-4.92 ± 0.23
	$\Delta E$	9.08 ± 2.17	$\Delta E$	11.77 ± 1.08	$\Delta E$	14.83 ± 1.89

Notes:  $\Delta L^*$ —black and white changes,  $\Delta a^*$ —red and green changes,  $\Delta b^*$ —yellow and blue changes,  $\Delta E$ —the overall color difference.

**Table 6.** Variation of Color Difference of four WPCs after Deionized Water Spray + Xenon Lamp Degradation Aging

WPC Type	Processing Days (d)					
	3		6		9	
Wheat straw/PVC	$\Delta L^*$	19.12 ± 1.2	$\Delta L^*$	29.89 ± 0.12	$\Delta L^*$	35.0233 ± 0.86
	$\Delta a^*$	2.25 ± 0.35	$\Delta a^*$	3.82 ± 0.45	$\Delta a^*$	1.077 ± 0.95
	$\Delta b^*$	5.93 ± 0.85	$\Delta b^*$	7.52 ± 1.23	$\Delta b^*$	-0.59 ± 0.62
	$\Delta E$	20.56 ± 1.32	$\Delta E$	31.11 ± 1.07	$\Delta E$	35.13 ± 1.19
Rice straw/PVC	$\Delta L^*$	15.13 ± 0.63	$\Delta L^*$	20.15 ± 0.75	$\Delta L^*$	32.23 ± 1.22
	$\Delta a^*$	-4.97 ± 1.2	$\Delta a^*$	-2.90 ± 0.41	$\Delta a^*$	-5.31 ± 0.46
	$\Delta b^*$	-10.14 ± 0.41	$\Delta b^*$	-10.23 ± 0.83	$\Delta b^*$	-14.33 ± 0.94
	$\Delta E$	19.03 ± 1.34	$\Delta E$	22.86 ± 1.09	$\Delta E$	35.71 ± 1.71
Reed/PVC	$\Delta L^*$	11.92 ± 0.84	$\Delta L^*$	11.04 ± 0.95	$\Delta L^*$	31.93 ± 1.41
	$\Delta a^*$	1.65 ± 0.27	$\Delta a^*$	2.10 ± 0.3	$\Delta a^*$	2.71 ± 0.57
	$\Delta b^*$	-11.05 ± 0.63	$\Delta b^*$	-11.69 ± 0.56	$\Delta b^*$	-12.13 ± 1.26
	$\Delta E$	11.76 ± 0.98	$\Delta E$	16.24 ± 1.25	$\Delta E$	34.28 ± 1.27
Bamboo/PVC	$\Delta L^*$	5.64 ± 0.58	$\Delta L^*$	7.97 ± 1.36	$\Delta L^*$	11.17 ± 1.18
	$\Delta a^*$	-1.6 ± 0.33	$\Delta a^*$	-1.22 ± 0.11	$\Delta a^*$	-1.03 ± 0.2
	$\Delta b^*$	-5.69 ± 0.27	$\Delta b^*$	-5.35 ± 0.37	$\Delta b^*$	-6.02 ± 0.17
	$\Delta E$	8.20 ± 0.76	$\Delta E$	9.85 ± 1.53	$\Delta E$	12.77 ± 1.42

Notes:  $\Delta L$ —black and white changes,  $\Delta A$ —red and green changes,  $\Delta B$ —yellow and blue changes,  $\Delta E$ —the color difference.

### Analysis of Water Absorption of Wood-Plastic Composites after Degradation Aging

Figure 3 shows the water absorption of four wood-plastic composites before and after degradation aging. The water absorption of the four wood-plastic composites increased with increased degradation aging time. The water absorption of reed/PVC composites and bamboo powder/PVC composites was similar, while the water absorption

of reed/PVC composites was the lowest. After 9 days of simulated seawater immersion + xenon lamp degradation aging and after 9 days of deionized water spray + xenon lamp degradation aging, its water absorption rates were 3.09% and 3.02%, respectively. The water absorption rate of wheat straw/PVC composite material and rice straw/PVC composite material was similar, and their water absorption and reed/PVC composite water absorption rate difference was about 1%. While the straw stalk/PVC composites had the highest water absorption rate, the water absorption rates after simulated seawater immersion + xenon lamp and deionized water spray + xenon lamp degradation aging for 9 days were 4.46% and 3.87%, respectively. The comparison shows that the water absorption rate of wood-plastic composites after simulated seawater immersion + xenon lamp degradation aging was higher than that after deionized water spray + xenon lamp degradative aging. The reason is that simulated seawater degradation and xenon lamp aging cause complex reactions such as photooxidation and degradation of composite materials, causing degradation of PVC and loss of plant fibers. At the same time, the defects such as cracks caused by the difference in surface polarity between the fiber and the PVC joint surface will be enlarged, and the hydrophilic groups in the plant fiber are more easily contacted with water. Compared with deionized water spray + xenon lamp degradation aging, the deterioration of wood-plastic composites after seawater immersion + xenon lamp aging was higher, and there were more internal defects. The difference in water absorption between wood-plastic composites after the two experiments was approximately 0.5%.

Figure 3 shows that the composite materials prepared from wheat straw, rice straw, and PVC had higher water absorption, and the composite materials prepared from reed, bamboo powder, and PVC had lower water absorption rate. The water absorption rate of reed/PVC composite material had the smallest change. The water absorption rate of bamboo powder/PVC composites varied the most because the reed and bamboo powder have higher cellulose content and higher crystallinity. Therefore, the hydrophilic hydroxyl groups contained in each other which is expressed according to the chemical composition of the four plant fibers.

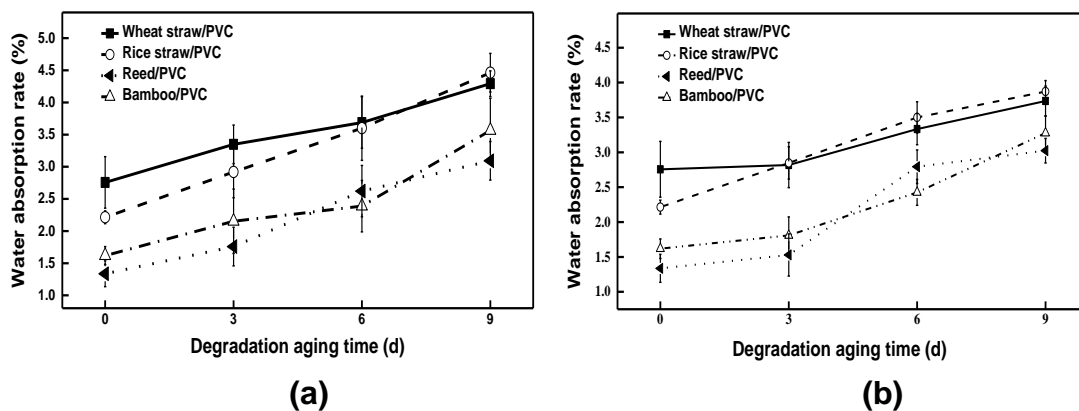


**Fig. 3.** The water absorption of wood-plastic composites after (a) simulated seawater immersion + xenon lamp degradation aging and (b) deionized water spray + xenon lamp degradation aging

Since the polarity is low, it is tightly combined with PVC, and it is difficult to contact with water molecules. The wheat straw plant had higher total cellulose content, and the fiber crystallinity was lower. The free hydroxyl content was relatively high, and it was easy to combine with water molecules so that hydrogen bonds were formed. The water absorption was relatively high, and the content of cellulose and hemicellulose in bamboo

powder was the highest. After aging degradation, a large amount of fiber was exposed to PVC, and the polarity of plant fiber itself was restored. Thus, the water absorption rate changed.

### Degradation Aging FTIR Analysis of Four Wood-plastic Composites

Figure 4 shows the infrared spectra of four plant fiber / PVC composites. The FTIR spectra of the four composite materials had different degrees of change after degradation aging, which were mainly manifested as differences in absorption peaks. The 3200 to 3400  $\text{cm}^{-1}$  band in the spectral curve shows hydroxyl vibration, which mainly comes from cellulose. After deionized water spray + xenon lamp degradation aging and simulated seawater immersion + xenon lamp degradation aging, the peaks of the four composite materials increased in the range of 3200 to 3400  $\text{cm}^{-1}$ , indicating an increase in hydroxyl content (Fabiya and McDonald 2010). The peak change after simulated seawater immersion + xenon lamp degradation and aging was more obvious than that after deionized water spray + xenon lamp degradation and aging. The exposed part of cellulose and hemicellulose caused an increase in -OH content. In addition, the characteristic absorption peaks of the four PVC-based wood-plastic composites before simulating seawater degradation were also strengthened after simulating seawater degradation, such as the asymmetric vibration peaks of methylene- $\text{CH}_2$ - in the PVC molecule (located at 2925  $\text{cm}^{-1}$  and 2870  $\text{cm}^{-1}$ ), in-plane shear vibration peaks (located at 1472  $\text{cm}^{-1}$  and 1460  $\text{cm}^{-1}$ ) and in-plane rocking vibration peaks (located at 730  $\text{cm}^{-1}$  and 718  $\text{cm}^{-1}$ ) (Hu 2013), indicating the simulation seawater degradation also leads to the breakage of PVC molecular chains.

At the same time, the change of the peak vibration at 1700  $\text{cm}^{-1}$  after degradation and aging of wood-plastic composite materials has the following reasons: (1) During the preparation of the wood-plastic composite material, plant fibers and PVC carbonyl groups were incorporated into the PVC matrix. The material absorbs incident light and initiates dehydrochlorination under ultraviolet light, resulting in photodegradation (Matuana *et al.* 2001, 2011). (2) Lignin contains an aromatic structure (chromophoric group) that absorbs ultraviolet light. Under photooxidation, the group degrades to produce products containing carboxyl and carbonyl groups. (3) Cellulose macromolecules react with oxygen to produce cellulose oxides and hydroperoxides. Two substances decompose to form ketone groups, enhancing the carbonyl peak. Therefore, the increased carbonyl content reflected the degree of degradation of the composite material. The increase of non-conjugated carbonyl groups (1734  $\text{cm}^{-1}$ ) and conjugated carbonyl groups (1637  $\text{cm}^{-1}$ ) was apparent on the surface of the material; the increase of non-conjugated carbonyl groups is attributed to the oxidation of hemicellulose of plant fibers in the photochemical reaction and the C—O bond is oxidized to produce C = O (Durmaz *et al.* 2019). The increase of the conjugated carbonyl group is mainly due to the cleavage of the  $\beta$ -O bond in lignin, and a quinoid structure is generated on the aromatic ring. Lignin was destroyed (1508, 1462  $\text{cm}^{-1}$ ) and part of the C—O—H bond on the guaiacyl aromatic ring was broken (1240  $\text{cm}^{-1}$ ).  $\text{CH}_2$  (1425  $\text{cm}^{-1}$ ), CH (1375  $\text{cm}^{-1}$ ), and C—O—C (1163  $\text{cm}^{-1}$ ) bonds were broken. At the same time, part of  $\beta$ -(1,4)-glycosidic bond in cellulose was broken (1103  $\text{cm}^{-1}$ ). After aging, free radicals and oxygen bridge and crosslink to cause C—O—C oxidation crosslinking vibration peak (1024  $\text{cm}^{-1}$ ) (Jiang 2019), vinyl C—H bending vibration in PVC (970 $\text{cm}^{-1}$ ), and the C—Cl stretching vibration peak (760  $\text{cm}^{-1}$  – 550  $\text{cm}^{-1}$ ) was weakened; that is, the material had degraded.

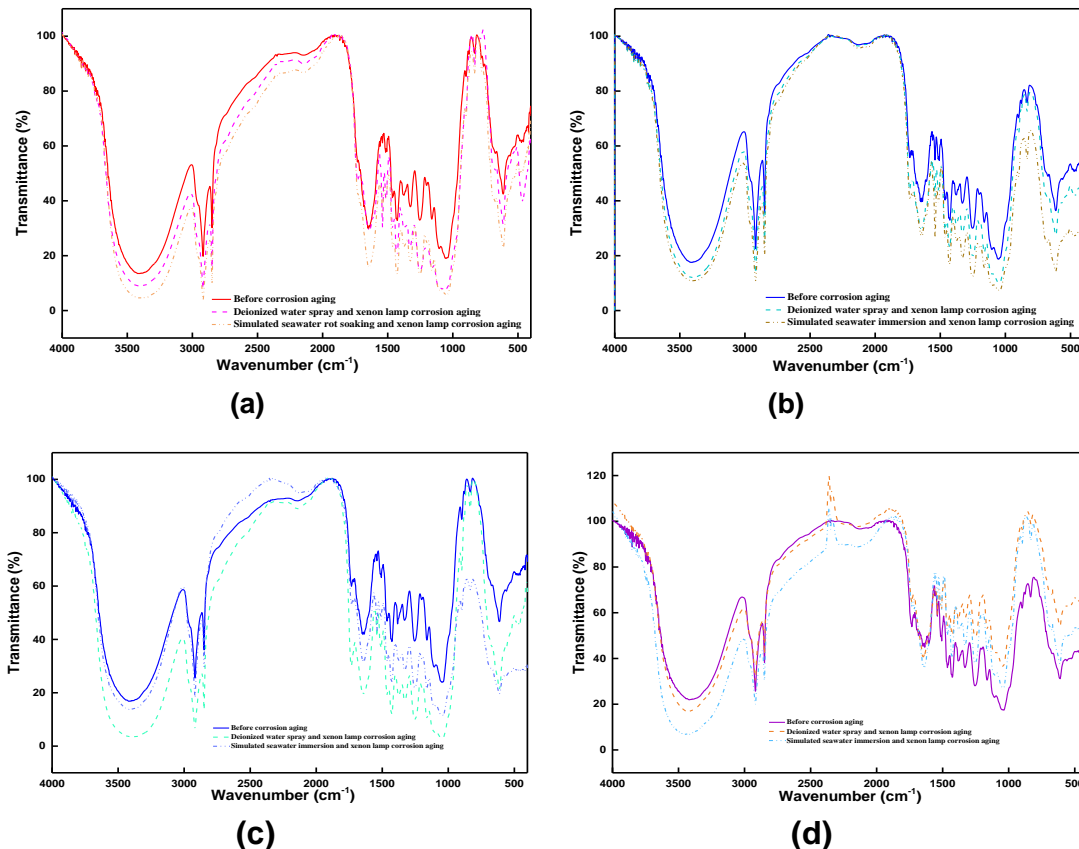


**Fig. 4.** FTIR spectra of (a) rice straw/PVC composite, (b) reed/PVC composite, (c) wheat straw/PVC composite, and (d) bamboo/PVC composite

### Microstructural Analysis of Four Wood-plastic Composites

Figure 5 shows the microstructure of four wood-plastic composites before degradation aging, after deionized water spray + xenon lamp degradation aging, and after simulated seawater immersion + xenon lamp degradation aging. The interface compatibility of the two phases of reed/PVC composites before degradation aging was the best. The internal bonding was tight, and the gaps and other defects were less. The straw/PVC composites had poor interfacial compatibility and there were small gaps. The reason is that the reed cellulose content is higher (Yu *et al.* 2015; Liu *et al.* 2016). The reed fiber has higher crystallinity. The surface polarity is lower. The plant fiber is tightly combined with PVC and the straw stalk/PVC composite material is the opposite, in a certain cellulose content range. The increase in cellulose content will cause fiber-matrix adhesion, which strengthens mechanical properties, and the interfacial bonding of the two phases is better (Shebani *et al.* 2009). After simulating seawater immersion + xenon lamp degradation aging and deionized water spray + xenon lamp degradation aging, wood-plastic composites had different degrees of defects. For wood-plastic composites with high crystallinity, the probability of defects was low and the performance was better. At the same time, the bonding interface between plant fibers and plastic matrix in plant fiber/PVC composites controls the stress transfer between fibers and matrix. The surface shape of plant fibers is irregular. During the formation of wood-plastic composites, PVC is infiltrated on the uneven surface of the plant fiber, such as peaks, valleys, cracks or other irregular shapes on the surface and mechanically locked to the plant fibers by adhesion. The fiber and the substrate are not easy to move relative to each other. The stress transfer

efficiency is high, and the mechanical interlocking phenomenon is strong (Zhou *et al.* 2016). Figure 5 shows that the surface shape of bamboo powder and reed fiber was irregular, and the mechanical interlocking effect with PVC was high. The mechanical properties of the formed wood-plastic composite material were relatively high, which is consistent with the mechanical properties.

Figure 5 shows an increase in the internal defects of the composite material after deionized water spray + xenon lamp degradation aging and simulated seawater immersion + xenon lamp degradation aging. A large number of cracks and voids appear in the cross section, and the plant fiber is separated from the PVC package, exposed to the outside. After simulated seawater immersion + xenon lamp degradation aging, the defects of wood-plastic composites were more than that of deionized water spray + xenon lamp after degradation and aging.

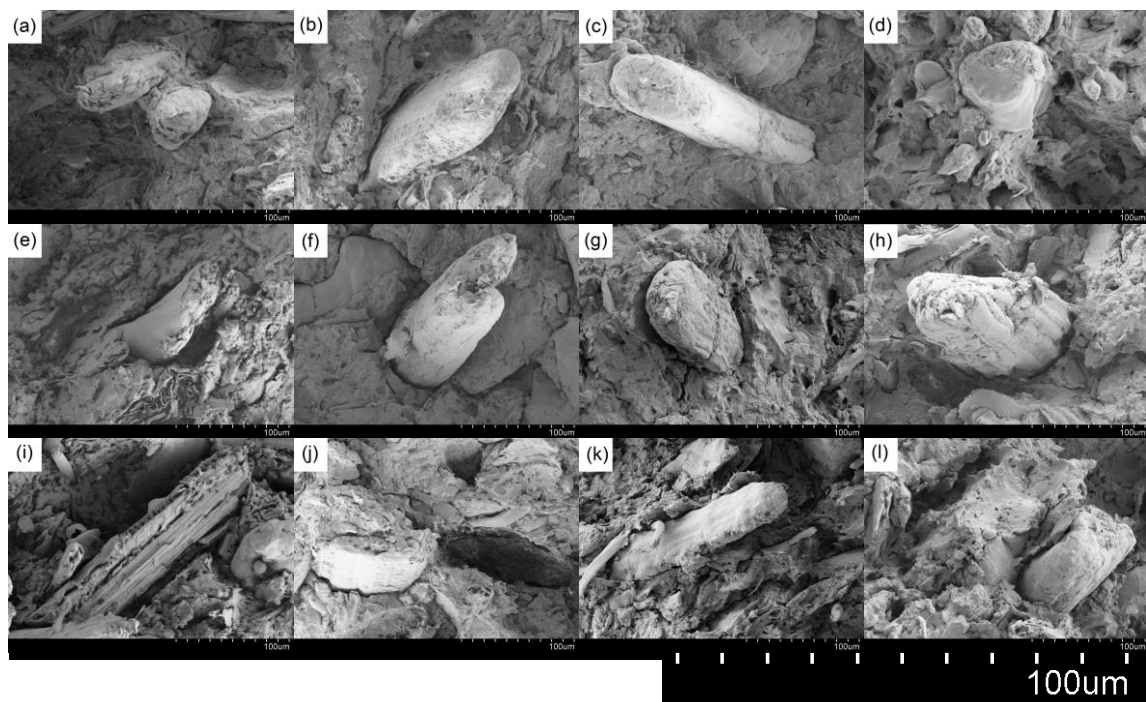


**Fig. 5.** Micro-morphology of four wood-plastic composites, including wheat straw/PVC, rice straw/PVC, reed/PVC and bamboo/PVC composites (a) (b) (c) (d) before degradation aging, (e) (f) (g) (h) after deionized water spray + xenon lamp degradation and aging and (i) (j) (k) (l) after simulated seawater immersion + xenon lamp degradation aging.

The xenon lamp aging simulated seawater degradation results in a reduction of the two-phase mass and increases the crack. At the same time, simulated seawater causes the plant fibers to swell, such that the fibers are exposed to the outside without PVC coated, and the gap between the plant fibers and the PVC is increased and the number is increased. Parts of exposed plant fibers are completely peeled off, and the simulated seawater color after soaking the wood-plastic composite material is deepened. After deionized water spray + xenon lamp degradation aging, the wood-plastic composite material only undergoes photochemical reaction under the aging effect of xenon lamp, which causes the quality of the two-phase combination of wood-plastic composite material to deteriorate. While the crack increases, the plant fiber does not leave the PVC matrix, and the degree of deterioration is smaller.

## CONCLUSIONS

1. Of the four kinds of plant fiber/PVC composites, the composite mechanical properties of reed/PVC composites were the best, and the comprehensive mechanical properties of straw/PVC composites were poor. After degradation aging, the comprehensive mechanical properties of reed/PVC composites were better. The mechanical properties of bamboo powder/PVC composites exhibited the smallest decrease.
2. The bamboo powder/PVC composite material had the smallest changes in color after degradation aging due to its light color. The  $\Delta E$  value was less than 14.8, and the  $\Delta E$  value of the reed/PVC composite material was between 34 and 38. The water absorption of the reed/PVC composites before and after degradation aging was lower than that of the other three composite materials.
3. After the simulated seawater immersion + xenon lamp degradation aging, the internal structure deterioration of the four wood-plastic composite materials was more serious. The internal cracks, holes, and other defects increase, and the combined quality of fiber and PVC was reduced. With a higher crystallinity of reed plant fiber, there was a lower content of active hydroxyl groups and tighter combination with PVC matrix. With less internal defects, there was better comprehensive performance of wood-plastic composites after degradation aging.

## ACKNOWLEDGMENTS

The work was financially supported by the National College Student Innovation Training Program (China, No. 20181037086).

## REFERENCES CITED

- GB/T 1040.1 (2006). "Determination of tensile properties of plastics," Standardization Administration of China, Beijing, China.
- GB/T 1451 (2005). "Determination of impact properties of plastic simply supported beams," Standardization Administration of China, Beijing, China.
- GB/T 17657 (2013). "Test methods evaluating the properties of wood-based panels and surface decorated wood-based panels," Standardization Administration of China, Beijing, China.
- GB/T 9341 (2008). "Determination of bending properties of plastics," Standardization Administration of China, Beijing, China.
- Deka, B. K., Mandal, M., and Maji, T. K. (2012). "Effect of nanoparticles on flammability, UV resistance, biodegradability, and chemical resistance of wood polymer nanocomposite," *Industrial & Engineering Chemistry Research* 51, 11181-11189. DOI: 10.1021/ie3003123
- Durmaz, S., Özgenç, Ö., Avci, E., and Boyaci, İ. H. (2019). "Weathering performance of waterborne acrylic coating systems on flat-pressed wood-plastic composites," *Journal of Applied Polymer Science* 10, 48518. DOI: 10.1002/app.48518
- Fabiyi, J. S., and McDonald, A. G. (2010). "Effect of wood species on property and weathering performance of wood plastic composites," *Composites Part A: Applied*

- Science and Manufacturing* 41(10), 1434-1440. DOI: 10.1016/j.compositesa.2010.06.004
- Fu, J. J., He, C. X., Jiang, C. Y., and Chen, Y. S. (2019). "Degradation resistance of alkali-treated eucalyptus fiber reinforced high density polyethylene composites as function of simulated sea water exposure," *BioResources* 14(3), 6384-6396. DOI: 10.15376/biores.14.3.6384-6396
- Hao, J. X., and Wang, W. H. (2016). "Application of wood-plastic composite materials in building formwork," *Forest Engineering* 3, 44-46. DOI: 10.16270/j.cnki.slgc.2016.03.010
- Hou, R. L., He, C. X., Xue, J., Yu, W., and Dou, C. C. (2013). "Ultraviolet accelerated aging properties of wheat straw powder/PP wood-plastic composites," *Acta Materiae Compositae Sinica* 30(05), 86-93. DOI: 10.13801/j.cnki.fhclxb.2013.05.021
- Hu, H., Wu, Z. K., Wang, Y., Guan, C., and Wang, W. (2013). "Study on the aging properties of wood-plastic composites," *Journal of Anhui Agricultural Science* 41(9), 3956-6957, 3993.
- Jiang, L. P., He, C. X., Fu, J. J., and Xu, D. Z. (2019). "Enhancement of wear and degradation resistance of polyvinyl chloride/sorghum straw-based composites in cyclic sea water and acid rain conditions," *Construction and Building Materials* 223, 133-141. DOI: 10.1016/j.conbuildmat.2019.06.216
- Jiang, L. P., He, C. X., Wang, L., and Jiang, C. Y. (2019). "Comparison of seawater degradation resistance of four plant fiber/high density polyethylene wood-plastic composites," *Acta Materiae Compositae Sinica* 2019, 36. DOI: 10.13801/j.cnki.fhclxb.20181023.001
- Matuana, L. M., Kamdem, D. P., and Zhang, J. (2001). "Photoaging and stabilization of rigid PVC/wood-fiber composites," *Journal of Applied Polymer Science* 80(11), 1943-1950. DOI: 10.1002/app.1292
- Matuana, L. M., Jin, S., and Stark, N. M. (2011). "Ultraviolet weathering of HDPE/wood-flour composites coextruded with a clear HDPE cap layer," *Polymer Degradation and Stability* 96, 97-106. DOI: 10.1016/j.polymdegradstab.2010.10.003
- Li, D. F. (2013). *Study on Performance Influence Factors and Interfacial Characteristic of PE Wood Plastic Composite*, Ph.D. Dissertation, Beijing Forestry University, Beijing, China.
- Li, Y., Liu, J. Z., Zhang, Y., Liu, T., and Zhou, Y. S. (2014). "Study on anti-aging properties of PVC-based wood-plastic composites," *Engineering Plastics Application* 42(06), 79-82. DOI: 10.3969/j.issn.1001-3539.2014.06.018
- Liu, D. N., He, C. X., Chang, X. N., Fu, J. J., and Wang, M. (2016). "Properties of PVC/straw fiber composites," *Engineering Plastics Application* 44(10): 6-11. DOI: 10.3969/j.issn.1001-3539.2016.10.002
- Qi, R., He, C., and Jin, Q. (2019). "Effect of acrylate-styrene-acrylonitrile on the aging properties of eucalyptus/PVC wood-plastic composites," *BioResources*. 14(4), 9159-9168. DOI: 10.15376/biores.14.4.9159-9168
- Rouhou, M. C., Abdelmoumen, S., Thomas, S., Attia, H., and Ghorbel, D. (2018). "Use of green chemistry methods in the extraction of dietary fibers from cactus rackets (*Opuntia ficus-indica*): Structural and microstructural studies," *International Journal of Biological Macromolecules* 116, 901-910. DOI: 10.1016/j.ijbiomac.2018.05.090
- Najafi, S. K., and Kordkheili, H. Y. (2011). "Effect of sea water on water absorption and flexural properties," *European Journal of Wood and Wood Products* 69(4), 553-556. DOI: 10.1007/s00107-010-0518-7

- Pan, H., Ni, M. Y., Jian, W. C., and Xu, C. Y. (2013). "Factors influencing the aging performance of wood-plastic composites," *Forestry Machinery and Woodworking Equipment* 2, 22-25.
- Segovia, F., Salvador, M.D., Sahuquillo, O., and Vicente, A. (2007). "Effects of long-term exposure on E-glass composite material subjected to stress. Degradation in a saline medium," *Journal of Composite Materials* 41(17), 2119-2128. DOI: 10.1177/0021998307074134
- Shebani, A. N., Van Reenen, A. J., and Meinckens, M. (2009). "The effect of wood species on the mechanical and thermal properties of wood-LLDPE composites," *Journal of Composite Materials* 43(11), 1305-1318. DOI: 10.1177/0021998308104548
- Sun, Z. Y., Li, D. G., Wu, Z. Y., and Ge, J. (2005). "Effect of artificial simulated seawater and acid rain on properties of wood/plastic composite," *Journal of China Plastics Industry* 33, 156-158. DOI: 10.3321/j.issn:1005-5770.2005.z1.045
- Tang, F. P. (1989). "The characteristic reaction profiles of photo-degradation and photo-oxidation within R-PVC thick samples," *Journal of Polymer Materials Science and Engineering* (02), 63-68. DOI: 10.16865/j.cnki.1000-7555.1989.02.010
- Xiao, W., and Li, D. G. (2010). "The effect of xenon lamp accelerated aging on the bending strength and elastic modulus of composite materials," *Journal of Forestry Machinery & Woodworking Equipment* 9(9), 37-39.
- Ye, J. D. (2018). "Application of wood plastic material in modern architectural landscape design," *Journal of Green Science and Technology* 19, 20-21. DOI: 10.16663/j.cnki.lskj.20181025.001
- You, K. (2016). "Design of public facilities-based WPC," *Journal of Guangdong Chemical Industry* 8, 109-110.
- Yu, H., Wang, H., Ye, X. D., Shao, Q., and Sheng, K. C. (2015). "Hydrothermal modification of bamboo fiber particle and its influence on bamboo-fiber-reinforced PVC composite," *Journal of Forestry Science & Technology Development* 29(05), 77-80. DOI: 10.13360/j.issn.1000-8101.2015.05.020
- Zhou, Y. H., Fan, M. Z., and Chen, L. H. (2016). "Interface and bonding mechanisms of plant fiber composites: An overview," *Journal of Composites Part B: Engineering* 101, 31-45. DOI:10.1016/j.compositesb.2016.06.055
- Zor, M., Can, A., and Gardner, D. J. (2019). "Surface characterization of weathered and heat-treated wood-based composites reinforced by styrene maleic anhydride," *Color Res. Appl.* 44, 1017-1023. DOI: 10.1002/col.22417

Article submitted: August 5, 2019; Peer review completed: Feb. 22, 2020; Revised version received and accepted: April 15, 2020; Published: May 4, 2020.

DOI: 10.15376/biores.15.3.4672-4688